doi:10.1016/S0022-2836(02)00564-8 available online at http://www.idealibrary.com on IDEAL® J. Mol. Biol. (2002) 320, 1087–1094

JMB

Structural Enzymology of Li^+-sensitive/Mg^{2+}-dependent Phosphatases

S. Patel[1], M. Martínez-Ripoll[2], Tom L. Blundell[1] and A. Albert[2]*

[1]*Department of Biochemistry University of Cambridge Tennis Court Road, Cambridge CB2 1GA, UK*

[2]*Grupo de Cristalografía Macromolecular y Biología Estructural, Instituto de Química Física "Rocasolano" Consejo Superior de Investigaciones Científicas Serrano 119, E-28006 Madrid Spain*

**Corresponding author*

Li^+-sensitive/Mg^{2+}-dependent phosphatases have attracted considerable attention since they have been proposed as targets for lithium therapy in the treatment of manic-depressive patients. The members of this enzyme superfamily display low levels of sequence identity while possessing a common fold and active site. Extensive structural and biochemical data demonstrate the direct involvement of two metal ions in catalysis, and show that lithium exerts its inhibitory action by blocking the products at the active site. By exploiting the different inhibitory properties of magnesium and calcium, we have been able to solve the X-ray structures of the Li^+-sensitive/Mg^{2+}-dependent 3′-phosphoadenosine-5′-phosphatase in complex with its substrate and with its products. The structural comparison of these complexes provides a 3D picture of the different stages of the catalytic cycle. This gives new insights into the understanding of the biological function of this group of enzymes and their lithium inhibition, and should assist in the design of improved inhibitors of therapeutic value.

Keywords: inositol; 3′-phosphoadenosine-5′-phosphate; lithium therapy; protein crystallography

Introduction

Li^+-sensitive/Mg^{2+}-dependent phosphatases (LiMgPPases) comprise a group of evolutionarily related enzymes that exhibit an absolute requirement for divalent metal ions and are inhibited by lithium.[1] They are well characterized and they include putative targets for lithium therapy in the treatment of manic-depressive patients.[2] LiMgPPases include fructose-1,6-bisphosphate 1-phosphatases (FBPases), inositol polyphosphate 1-phosphatases (IPPases), inositol monophosphatases (IMPases), 3′-phosphoadenosine-5′-phosphatases (PAPases) and enzymes acting on both inositol-1,4-bisphosphate and PAP (PIPases).[3] Extensive structural and kinetic investigations[4,5] show that they possess a common structural core with the active site, including two or three metal-binding sites, lying between α + β and α/β domains.

The catalytic mechanism of LiMgPPases has been the subject of discussion for many years. Of particular interest is the question as to which of the bound metals provides the activation of the nucleophilic water molecule. Bone *et al*. suggested that the metal bound at site 1 would chelate the water molecule and that the mechanism would proceed *via* in-line nucleophilic displacement with inversion of configuration at phosphate.[6] Bone *et al*. suggested that a magnesium ion at site 1 and a Thr residue are responsible for the activation of the water molecule.[6] In this mechanism, another magnesium ion at site 2 is assumed to assist in phosphate coordination and charge stabilization during the transition state. On the other hand, Gani & Wilkie suggested that the activation of the nucleophilic water molecule occurs at site 2 and that the mechanism proceeds *via* adjacent association followed by pseudo-rotation with retention of configuration.[7] The determination of the stereochemical course of the reaction completely ruled out this mechanism.[8] However, Gani and

Present address: S. Patel, Astex Technology Ltd, 250 Cambridge Science Park, Milton Road, Cambridge, CB4 0WE, UK.

Abbreviations used: LiMgPPase, Li^+-sensitive/Mg^{2+}-dependent phosphatase; FBPase, fructose-1,6-bisphosphate 1-phosphatase; IPPase, inositol polyphosphate 1-phosphatase; IMPase, inositol monophosphatase; PAP, 3′-phosphoadenosine-5′-phosphate; PAPase, 3′-phosphoadenosine-5′-phosphatases; PAPS, 3′-phosphoadenosine-5′-phosphosulphate; PIPases, enzymes acting on both inositol-1,4-bisphosphate and PAP; CSD, the Cambridge Structural Database.

E-mail address of the corresponding author: xalbert@iqfr.csic.es

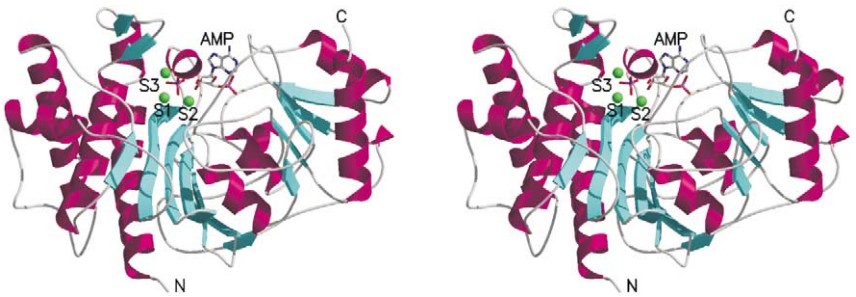

Figure 1. Ribbon representation of the Hal2p–Mg complex. α-Helices are colored magenta and beta strands are colored cyan. N and C termini, the three magnesium sites and the AMP molecule are labeled. Magnesium ions, AMP and Pi molecules are displayed in ball-and-stick mode. S1, S2 and S3 stand for the metal-binding sites 1, 2 and 3, respectively.

collaborators provided significant experimental evidence to suggest that site 2 does more than just serve as a Lewis acid.[7,9] Despite this detailed kinetic and structural information, some details of the mechanism remain obscure. It is not clear how many metal ions are required for the activation of the nucleophilic water molecule, and their precise role in the catalytic cycle is not understood. The molecular basis of the inhibition of this group of enzymes by lithium and other metal ions remains unclear.

Yeast PAPase, Hal2p, catalyses the hydrolysis of the 3′-phosphoadenosine-5′-phosphate (PAP) to adenosine-5′-phosphate (AMP). PAP is a side-product of the enzymes that use 3′-phosphoadenosine-5′-phosphosulphate (PAPS) as the activated sulfur source. The accumulation of intracellular PAP has the toxic effect of inhibiting this group of enzymes. This leads to the disruption of the sulfur assimilation pathway in yeast[10] and mammals.[11] In addition, PAP inhibits the RNA-processing enzymes[12] as it mimics the monomers of polyribonucleotide chain. Hal2p has attracted considerable interest, as it is an *in vivo* target for salt toxicity. Hal2p is inhibited by low concentrations of lithium and sodium.[10,13,14] Inhibition of Hal2p during salt stress abolishes cell survival. The enzyme is also non-competitively inhibited with respect to substrate by magnesium ions and competitively inhibited with respect to magnesium by calcium ions.[14]

Table 1. Data collection, structure solution and refinement statistics

	Hal2Mg	Hal2Ca
A. *Data collection*		
Space group	$P2_1$	$P2_1$
Cell parameters		
a, *b*, *c* (Å)	54.69, 45.08, 71.79	54.88, 44.97, 72.11
β (deg.)	110.96	110.72
Wavelength (Å)	1.5418	0.8700
Resolution limits (Å)	20–1.9	50–1.3
Multiplicity	3.2	2.9
Completeness (all data) (%)	99 (97)	90 (77)
Average $I/\sigma(I)$ (highest resolution shell)	5.6 (1.8)	16.4 (2.1)
R_{meas}[a]	0.09(0.41)	0.08(0.45)
B. *Crystallographic refinement*		
Resolution range (Å)	20–1.9	50–1.3
R_{free}	0.205	0.169
R_{factor}	0.151	0.133
No. reflections for refinement	24,591	69,524
No. parameters	11,992	26,541
C. *Final model parameters*		
Residues	354	354
Hetero groups	3	3
No. Water molecules	239	450
Average *B*-factor, protein (Å^2)	21.4	13.4
Average *B*-factor, water molecules (Å^2)	29.2	28.4
Model quality		
Ramachandran plot (% residues)		
In most favoured regions	90.4	89.2
In generously allowed regions	9.2	10.5
In disallowed regions	0.3	0.3
RMS deviations from ideal		
Covalent bond lengths (Å)	0.021	0.016
Bond angle (deg.)	3.2	1.7
Planar groups (Å)	0.008	0.008

[a] Multiplicity weighted R_{sym}:[33] $R_{meas} = [\sum_h \sqrt{n_h/(n_h-1)}\sum_i |\hat{I}_h - I_{h,i}|]/\sum_h \sum_i I_{h,i}$, $\hat{I}_h = (1/n_h)\sum_i^{n_h} I_h$. Highest-resolution shell for each dataset (Å): Hal2Ca (1.37–1.30) and Hal2Mg (2.02–1.90).

Table 2. Coordination geometry of Li–oxygen, Mg–oxygen and Ca–oxygen complexes found in the CSD and in Hal2p active site

	Distance Me–O	Angle O–Me–O	Coordination geometry	No. observations
CSD				
$Li–O_4$	1.95(0.06)	110(12)	Tetrahedral/distorted squared	529
$Mg–O_6$	2.07(0.04)	88(6)/179(2)	Octahedral	268
$Ca–O_6$	2.33(0.06)	89(8)/179(5)	Octahedral	77
Hal2p–Mg complex				
$Mg(1)–O_6$	2.10(0.09)			
$Mg(2)–O_6$	2.11(0.18)			
$Mg(3)–O_6$	2.14(0.15)			
Hal2p–Ca complex				
$Ca(1)–O_6$	2.34(0.05)			
$Mg(2)–O_6$	2.18(0.12)			

All distances are given in Å. The sample standard deviations (SD) are in parentheses.

The X-ray structure of Hal2p at high resolution revealed that lithium exerts its inhibitory action by blocking the products of the PAP hydrolysis at the active site.[15] The structure provided a 3D picture of the metal-binding sites and of the products at the active site after the hydrolysis of PAP. Two magnesium ions (at sites 1 and 3), a molecule of AMP and a phosphate ion (Pi) were found in the active site. Both metal ions are octahedrally coordinated. Mg 1 coordinates Glu72 OG1, Asp142 OD1, Ile143 O, a water molecule (Wat3) and two oxygen atoms of Pi. Mg 3 coordinates Glu72 OG2, two oxygen atoms of Pi and three water molecules. A third metal-binding site was identified indirectly as the lithium-binding site. At this site, lithium is expected to be coordinated by AMP OH3′, Asp294 OD1, Asp 142 OD2 and an oxygen atom of Pi.

Using the different inhibitory properties of magnesium and calcium we have been able to solve the X-ray structures of the Hal2p in complex with substrate (PAP) and with products (AMP and Pi). The structural comparison of these complexes provides a 3D picture of the different stages of the hydrolysis of PAP. This supports the mechanism previously reported for PIPases and IMPases, and suggests that the same mechanism is applicable to the superfamily of enzymes. The structural analysis provides new insights into the role of different metal sites and into the molecular basis for lithium, calcium and magnesium inhibition.

Results

The X-ray structures of Hal2p in complex with magnesium and with calcium ions were solved at 1.90 Å and 1.30 Å resolution, respectively (see Figure 1, Table 1 and Materials and Methods).

Comparing the geometry of the stable compounds found in the Cambridge Structural Database (CSD)[16] with the stable or pre-reactive geometry observed in the Hal2p active site helps in understanding the roles of different metal ions and participants in the hydrolysis of PAP. Hence, the CSD was used to identify metal oxygen complexes and to analyze the sphere of coordination of lithium, magnesium and calcium metal ions (Table 2). In addition, we used the CSD to identify compounds containing hydroxyl (OH) and phosphate moieties (PO_4) with an O(OH)–P distance (d) below 3.6 Å (van der Waals distance plus 10%). The geometry of this system was described in terms of d and the largest O(OH)–P–O angle (attack angle, α). The distribution of d *versus* α clusters stable molecules into two groups: the first group includes the molecules with d values ranging from 1.6 to 1.7 Å and α values between 165° and 180°. These molecules correspond to a trigonal bipiramidal pentavalent phosphorus atom. The second group presents a d value greater than 3.2 Å and corresponds to non-covalent interactions between the hydroxyl group and phosphorus. The whole distribution seems to represent the two extreme cases of a nucleophilic substitution at a phosphate molecule *via* formation of a bipyramidal trigonal phosphate intermediate. There are no observations between these two clusters, since these angles and distances would imply a reactive state.

The electron density for the magnesium and calcium Hal2p complexes allowed unambiguous positioning of the protein side-chains throughout the structures (see Materials and Methods, and Table 2). Overall, the Hal2p models were very similar, with changes confined to the active-site regions (see Figure 2). A brief description of each complex is given below.

Magnesium complex

The X-ray structure of Hal2p in complex with magnesium helps to confirm the metal-binding site 2 that was not observed directly in the original structure of Hal2p (Figure 2(a) and (b)). On the other hand, the products of the hydrolysis of PAP, AMP and Pi, and the magnesium atoms at sites 1 and 3 remain at the active site. This is in agreement with the biochemical data showing that Hal2p is moderately inhibited by magnesium.[10] Hal2p crystals were soaked with an excess of magnesium. This may prevent magnesium at the active site from dissociation and, consequently, product

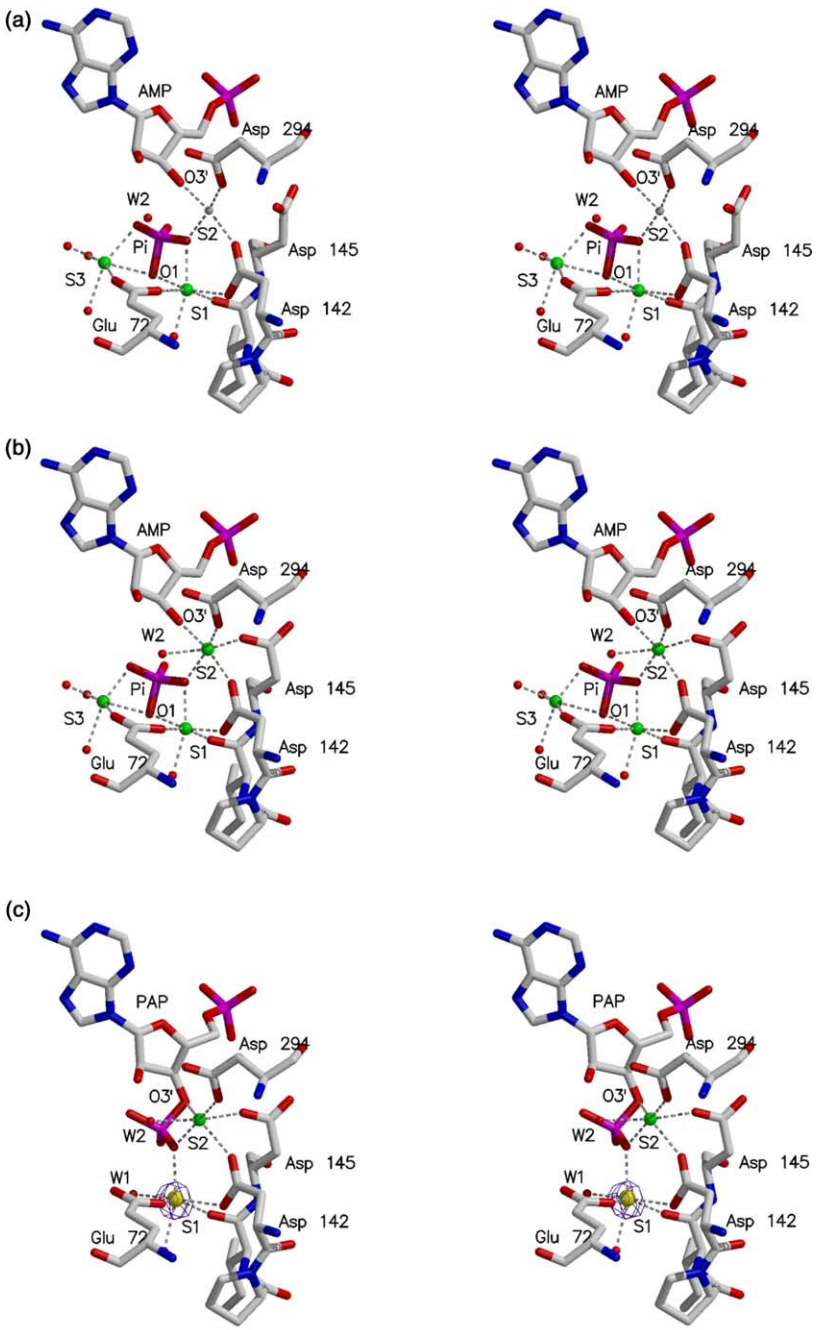

Figure 2. Stereo view of the metal-binding sites (a) in the Hal2p–lithium complex, (b) in the Hal2p magnesium complex, and (c) in the Hal2p–calcium complex. A section of the difference anomalous map at 5σ is also depicted in (c). Magnesium ions are colored green, the calcium ion is colored yellow and the putative lithium ion is colored gray. Coordinates of (a) are taken from PDB code 1QGX. S1, S2 and S3 stand for the metal-binding sites 1, 2 and 3, respectively.

release. Site 2 is occupied by a magnesium ion and displays octahedral geometry. This metal ion is coordinated to AMP O3′, Asp294 OD1, Asp142 OD2, Asp145 OD1, Wat2 and Pi O1. A comparison with the Hal2p original structure shows that Asp145 and Wat2 move to assist in coordinating magnesium at site 2, which now is bound to six ligands. This is in agreement with the data extracted from the CSD, where the most favored coordination numbers for lithium and magnesium are four and six, respectively. However, the observed distances and angles for Li–O and for Mg–O complexes are quite similar (see Table 2). Hence, one would expect that both lithium and magnesium would compete for site 2, as this site is able to accommodate either four or six ligands.

Calcium complex

The high-resolution electron density map at the active site of the Hal2p calcium complex unequivocally shows one calcium ion at site 1, one magnesium ion at site 2 and a molecule of the PAP substrate. Metal-binding site 3 appears to be empty (see Figure 2(c)). The binding of calcium at site 1 is in agreement with the biochemical data showing that calcium inhibits Hal2p competitively with respect to magnesium. Both magnesium and calcium ions are octahedrally coordinated. Despite the presence of the substrate PAP in the active site, the geometry of the metal-binding sites is only slightly different from that seen in previous structures (see Figure 2). At magnesium-binding

site 2, the AMP OH3′ is replaced with the equivalent oxygen atom O3′ of the PAP phosphoester bond. Consequently, the Pi O2 is replaced by a water molecule (Wat1) at calcium-binding site 1. This site displays metal–oxygen distances larger than those observed in the magnesium complex. This is in agreement with the distances found for the Ca–O complexes in the CSD (see Table 2). Anisotropic thermal parameters for protein atoms, ligand molecules and water, Wat1, were included in the final stages of the Hal2p calcium complex refinement. Interestingly, the analysis of the thermal parameters shows that Asp145 OD1 and OD2 present high anisotropy when compared with the rest of the active-site residues. This is in agreement with the ability of this residue to change its conformation upon binding of lithium or magnesium metal ions at site 2.

Discussion

Hal2p catalytic mechanism

The structures of the Hal2p–Ca PAP substrate complex (Ca-complex) and of the Hal2p–Mg AMP-Pi products complex (Mg-complex) mimic the intermediate states before and after the hydrolysis of PAP, respectively. Comparisons of these two structures and the previously reported structure of the Hal2p–Li AMP-Pi complex[15] (Li-complex) provide the position of all the participants in the catalytic mechanism; in effect they represent three-dimensional pictures of different stages of the catalytic cycle. The integration of these structural data with the data extracted from CSD and the mechanistic data based on the biochemistry and the structures of the members of the superfamily assists in understanding the role of the participants in the catalytic mechanism that drives the hydrolysis of PAP.

Activation of the nucleophilic water molecule

The Hal2p–Ca complex provides the first structural evidence of the existence of two water molecules in the vicinity of a non-hydrolyzed substrate molecule in a LiMgPPase. These water molecules are Wat1 at site 1 and Wat2 at site 2 (see Figure 2(c)).

The comparison of the geometry of the interaction between these water molecules and the phosphorus reaction center with the geometry of the stable analogous compounds found in the CSD helps in understanding the role of Wat1 and Wat2 in the catalytic cycle. The Wat1–PO_4 distance in the Ca-complex is slightly lower than the sum of the van der Waals distances for oxygen and phosphorus (3.2 Å). One would expect that the replacement of calcium by magnesium at site 1 would drive the system to a reactive state by decreasing the Wat1–phosphorus distance. In fact, the interaction between the phosphorus atom and the leaving O3′H oxygen atom observed in the Mg-complex displays reactive geometry, as it does not lie in either of the two stable clusters observed in CSD. On the other hand, the Wat2–PO_4 interaction observed in the Ca-complex, displays geometry similar to that observed for stable analogous compounds. Since the position of Wat2 is conserved in the Mg-complex, it is likely that the replacement of calcium by magnesium at site 1 does not affect the geometry of the interaction Wat2–PO_4. These structural data support that the view that the nucleophilic water molecule in the hydrolysis of the phosphoester bond is placed at Wat1, as proposed for other enzymes of the superfamilly.[5,6]

The activation of the Wat1 water molecule most likely derives from its interaction with magnesium at site 1 and from a framework of interactions that facilitates the transfer of a proton from Wat1 to Thr147 OG, and from this residue to Asp49 OD1 (see Figure 3(a)). Interestingly, this framework is conserved among the members of the LiMgPPase superfamily. In addition, previous mutagenic studies on the equivalent Thr residue of human IMPases[17] indicate a direct involvement of this residue in catalysis. The emerging hydroxyl ion at Wat1 would attack the phosphorus reaction center. Remarkably, the analysis of the thermal anisotropic factor for Wat1 shows that its highest displacement axis is in the direction of the phosphorus atom.

The Hal2p–Li and the Hal2p–Mg complexes and the crystal structures of the rat PIPase[5] and *Methanococcus jannaschii* IMPase/FRPase in complex with the phosphate product[18] suggest the involvement of a magnesium atom at site 3 in the activation of the nucleophilic water molecule. However, metal ions at site 3 display high thermal parameters and poorly defined water structure. This may be a consequence of the weak interaction between the metal ion and the protein, as the former is only bound to one protein atom. Hence, it is likely that this site is occupied if an excess of magnesium is available. In addition, these structures do not provide direct evidence of the interaction of a metal at site 3 and a water molecule at Wat1 in an enzyme substrate complex.

Hydrolysis of the phosphoester and product formation

The comparison of the structure of the substrate and of the Pi provided by the Ca-complex and the Mg-complex suggests that an inversion of the configuration occurs about the phosphorus atom. The Mg-complex provides the positions of the entering and leaving oxygen atoms after the nucleophilic displacement (Pi O2 and AMP O3′H respectively, see Figure 2(b)). The distance between these two atoms is 4.4 Å. This value is lower than twice the sum of the van der Waals distances of oxygen and phosphorus (6.4 Å); hence, the reaction mechanism should exhibit a strong associative character.[19] This implies the formation of a trigonal bipyramidal intermediate state at the phosphorus atom with the entering and the leaving oxygen atoms in

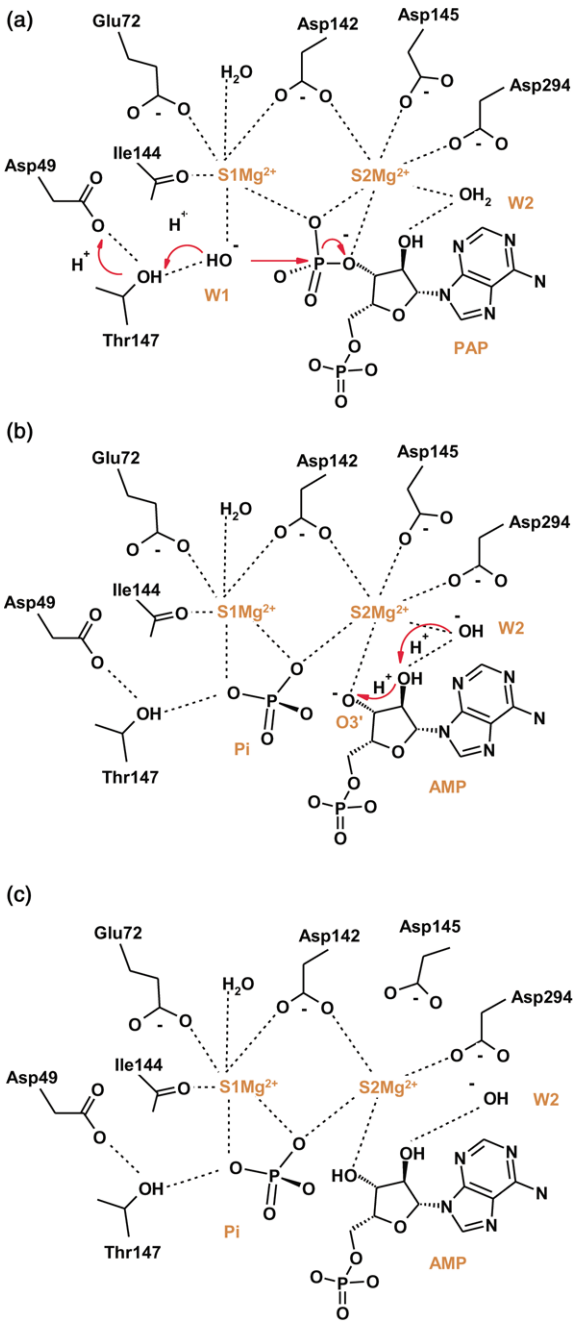

Figure 3. A diagram showing the different steps of the Hal2p reaction mechanism. (a) Activation of the catalytic water molecule and nucleophilic attack. (b) Products formation and protonation of the leaving group. (c) Charge stabilization and product release. The interactions displayed in the Figure are taken from Hal2p–calcium complex, Hal2p–magnesium complex and from Hal2p–lithium complex (PDB code 1QGX) for (a), (b) and (c), respectively.

apical positions. This intermediate would be anchored to the enzyme or to the magnesium ions by four direct interactions. In such a situation, the rotation of the product, Pi, will not be possible and, consequently, the hydrolysis of the phosphoester should involve an inversion of the configuration at the phosphorus atom.

Once the phosphoester bond is broken, the leaving AMP oxygen atom O3′ needs to be protonated. The only source of protons in the vicinity of this group is AMP O2′H (see Figure 3(b)). This oxygen atom is hydrogen bonded to Asp294 and to the water molecule Wat2. Asp294 would enhance the acceptor character of AMP O2′H and Wat2 could donate the required proton, since it is accessible to the solvent. This confers an essential role to Wat2 in the hydrolysis of PAP, since a failure in the protonation of the leaving AMP O3′ would drive the reaction equilibrium to the PAP substrate. There are several biochemical findings reported for inositol monophosphatase that support this hypothesis. Wilkie *et al.* were able to design potent competitive, non-hydrolysable inhibitors based on substrate-analogues lacking the equivalent PAP O2′H hydroxyl group or with a bulky group at this position that hinders the approach of the Wat2 water molecule.[20]

Product release

When the phosphoester is hydrolyzed, an excess of negative charge is generated at site 2 that the magnesium ion itself is not able to compensate (see Figure 3(b)). In order to dissipate this excess of charge, it is likely that the emerging hydroxyl group at Wat2 and Asp145 move apart from site 2. This rearrangement is observed in the Li-complex where neither Wat2 nor Asp145 is coordinating at site 2 (see Figure 3(c)).

The high thermal parameter and thermal anisotropy of Asp145 support this idea. The suggested reduction of the coordination number at site 2 (from six to four) would destabilize the magnesium at this site and would promote product release. Consequently, and in agreement with the biochemical data presented by Leech *et al.*, it is likely that the AMP product, which is coordinated to site 2, would leave the active site first, and Pi at site 1 last.[21]

Lithium inhibition

It has been suggested that lithium exerts its inhibitory action in LiMgPPases by blocking the products of substrate hydrolysis at the active site. The replacement at site 2 of the magnesium ion for a lithium ion stabilizes the tetra-coordinated complex formed after the hydrolysis of the substrate.[15] Cole *et al.* suggested that lithium would bind the enzyme after the catalysis has occurred.[9] However, there are several experimental findings arising from the comparison of the different Hal2p–metal complexes, indicating that the hydrolysis of the substrate can take place even if lithium is coordinating at site 2: first, lithium does not disrupt the coordination at site S1 and, consequently, the position of the nucleophilic water molecule. Second, as observed using the CSD, lithium binding does not produce a site rearrangement other than the reduction of the coordination number. Lithium would bind PAP in a productive

conformation, since this reduction does not imply substrate atoms and/or a substrate rearrangement. Finally, the interaction network involving Wat2, O2′H and O3′H is conserved in the Li-complex. Hence, lithium does not hinder protonation of products after hydrolysis of phosphoester.

In addition, kinetic studies showed that one magnesium ion is required for substrate binding and that lithium inhibits in an uncompetitive manner with respect to substrate and non-competitively with respect to magnesium cofactor.[2,3] Taking into account our structural findings and the biochemical data, it can be proposed that lithium binds to the ternary complex formed by Hal2p, magnesium binds at site 1 and the PAP substrate, before hydrolysis takes place.

Concluding remark

The structure of the Hal2p–metal complexes presented in this work provides a three-dimensional picture of the different stages of the catalytic cycle of the Li^+-sensitive/Mg^{2+}-dependent phosphatases. The comparison of these data with the previously reported structures of other members of the superfamily assists in understanding the role of both the different metal sites in the catalysis and the different metal ions as inhibitors. Consequently, the structural analysis provides new insights in the design of organic inhibitors for this group of enzymes.

Materials and Methods

Hal2p protein crystals were grown as described.[15] Separate mother liquor solutions (0.1 M sodium acetate, 0.1 M Mes (pH 6.5), 5 mM β-mercaptoethanol, 30% (w/v) PEG 5000 MME and 0.56 mM PAP) were made each containing 1 M magnesium chloride or 0.5 M calcium chloride. Crystals were incubated in 5 μl hanging-drops of the metal ion solutions for periods of between one and five hours, and subsequently transferred into mother liquor containing 20% (v/v) glycerol prior to cryo data collection.

The X-ray dataset for Hal2p–Mg was collected on an in-house Enraf Nonius rotating anode generator and a Mar345 detector with crystals cooled to 100 K using a CryoStream™ (Oxford CyroSytems Ltd). The Hal2-Ca dataset was collected on Station 9.6 of SRS (Daresbury, UK) with a Quantum 4 charge coupled device (CCD) detector (ADSC). In-house and SRS collected data were integrated with either DENZO[22] or MOSFLM;[23] data were scaled and merged using either SCALEPACK[22] or SCALA[24] and intensities were converted to amplitudes using TRUNCATE.[24]

The program MOLEMAN2[25] was used to remove a sphere of residues around the active site of Hal2p (PDB code 1QGX), water molecules and ligands were also ignored prior to ten cycles of rigid-body refinement and 20 cycles of restrained individual isotropic temperature factor refinement, using REFMAC5.[26] σ_A-weighted $2mF_o - DF_c$ and difference maps were calculated using FFT[24] and examined visually in the molecular graphics package O,[27] where all model rebuilding was performed. All the clearly visible protein main-chain and side-chain atoms were built into the electron density and any errors in side-chain atom positions elsewhere in the protein corrected. The rebuilt model was refined as before, using ten cycles of restrained individual isotropic temperature factor refinement and maps were recalculated. In addition, anomalous Fourier difference maps were calculated using FFT to help discriminate between different metal ions in the active site. Metal ions and active-site ligands were built into the electron density, short cycles of restrained isotropic refinement were performed and occupancies varied manually to optimize the match with the difference electron density. Finally, automated addition of ordered solvent molecules was performed by alternate cycles of ARP/wARP[28] and REFMAC5 until convergence of the R_{free}. For the Hal2–Ca dataset, where the resolution extended to 1.3 Å, restrained individual anisotropic temperature factor refinement of the protein and ligand atoms was attempted while treating temperature factors of the solvent molecules isotropically using the mixed option within REFMAC5.[26] Model quality assessments were made using PROCHECK[29] and WHATCHECK.[30] Ribbon figures were produced using MOLSCRIPT[31] and Raster3D.[32]

Protein Data Bank accession numbers

The coordinates and structure factors amplitudes of Hal2p in complex with magnesium and Hal2p in complex with calcium have been deposited in the RCSB Protein Data Bank with accession codes 1K9Y and 1KA1, respectively.

Acknowledgments

We thank Professor F. H. Cano for critical comments on the manuscript. S.P. was supported by a BBSRC earmarked studentship and for Astex CASE studentship. T.L.B. thanks the BBSRC Cambridge and East Anglia Structural Biology Centre for access to X-ray and computing equipment. Work in A.A.'s laboratory was funded by grants PB1998-0565-C04-04 of the Spanish "Plan Nacional" (CICYT, Madrid) and 08.5/0055./2000 of the Dirección General de Investigación de la Comunidad Autónoma de Madrid.

References

1. York, J. D., Ponder, J. W. & Majerus, P. W. (1995). Definition of a metal-dependent Li^+-inhibited phosphomonoesterase protein family based upon a conserved 3-dimensional core structure. *Proc. Natl Acad. Sci. USA*, **92**, 5149–5153.
2. Nahorski, S. R., Ragan, C. I. & Challiss, R. A. (1991). Lithium and the phosphoinositide cycle: an example of uncompetitive inhibition and its pharmacological consequences. *Trends Pharmacol. Sci.* **12**, 297–303.
3. Lopez-Coronado, J. M., Belles, J. M., Lesage, F., Serrano, R. & Rodriguez, P. L. (1999). A novel mammalian lithium-sensitive enzyme with a dual enzymatic activity, 3′-phosphoadenosine 5′-phosphate phosphatase and inositol-polyphosphate 1-phosphatase. *J. Biol. Chem.* **274**, 16034–16039.
4. Strater, N., Lipscomb, W. N., Klabunde, T. & Krebs, B. (1996). Two-metal ion catalysis in enzymatic acyl- and phosphoryl-transfer reactions. *Angew. Chem., Int. Ed. Engl.* **35**, 2024–2055.

5. Patel, S., Yenush, Y., Rodríguez, P. L., Serrano, R. & Blundell, T. L. (2002). Crystal structure of an enzyme displaying both inositol-polyphosphate 1-phosphatase and 3′-phosphoadenosine-5′-phosphate phosphatase activities: a novel target of lithium therapy. *J. Mol. Biol.* **315**, 677–685.
6. Bone, R., Springer, J. P. & Atack, J. R. (1992). Structure of inositol monophosphatase, the putative target of lithium-therapy. *Proc. Natl Acad. Sci. USA*, **89**, 10031–10035.
7. Gani, D. & Wilkie, J. (1995). Stereochemical, mechanistic, and structural features of enzyme-catalyzed phosphate monoester hydrolyzes. *Chem. Soc. Rev.* **24**, 55–63.
8. Faroux, C. M. J., Lee, M., Cullis, P. M., Douglas, K. T., Freeman, S., Gore, M. G. (1999). Inversion of configuration during the hydrolysis of D-1-Sp-myo-Inositol (17O) thiophosphate catalyzed by myo-Inositol monophosphatase. *J. Am. Chem. Soc.* **121**, 8385–8386.
9. Cole, A. G., Wilkie, J. & Gani, D. (1995). Probes for the position and mechanistic role of the 2nd catalytic magnesium-ion in the inositol monophosphatase reaction. *J. Chem. Soc., Perkin Trans. 1*, **21**, 2695–2707.
10. Murguia, J. R., Belles, J. M. & Serrano, R. (1995). A salt-sensitive 3′(2′),5′-bisphosphate nucleotidase involved in sulfate activation. *Science*, **267**, 232–234.
11. Roth, J. A., Rivett, A. J. & Renskers, K. J. (1982). Properties of human brain phenol sulfotransferase and its role in the activation of catecholamine neurotransmitters. In *Sulfate Metabolism and Sulfate Conjugation* (Mulder, G. J., Caldwell, J., Van Kempen, G. M. J. & Vonk, R. J., eds), pp. 107–114, Tailor and Francis, London, UK.
12. Dichtl, B., Stevens, A. & Tollervey, D. (1997). Lithium toxicity in yeast is due to the inhibition of RNA processing enzymes. *EMBO J.* **16**, 7184–7195.
13. Glaser, H. U., Thomas, D., Gaxiola, R., Montrichard, F., Surdun-Kerjan, Y. & Serrano, R. (1993). Salt tolerance and methionine biosynthesis in *Saccharomyces cerevisiae* involve a putative phosphatase gene. *EMBO J.* **12**, 3105–3110.
14. Murguia, J. R., Belles, J. M. & Serrano, R. (1996). The yeast HAL2 nucleotidase is an *in vivo* target of salt toxicity. *J. Biol. Chem.* **271**, 29029–29033.
15. Albert, A., Yenush, L., Gil-Mascarell, M. R., Rodriguez, P. L., Patel, S., Martinez-Ripoll, M. *et al.* (2000). X-ray structure of yeast Hal2p, a major target of lithium and sodium toxicity, and identification of framework interactions determining cation sensitivity. *J. Mol. Biol.* **295**, 927–938.
16. Allen, F. H., Davies, J. E., Galloy, J. J., Johnson, O., Kennard, O., Macrae, C. F. *et al.* (1991). The development of version-3 and version-4 of the Cambridge structural database system. *J. Chem. Info. Comput. Sci.* **31**, 187–204.
17. Pollack, S. J., Knowles, R., Broughton, H. B., Ragan, C. I., Osborne, S. A. & McAllister, G. (1993). Probing the role of metal-ions in the mechanism of inositol monophosphatase by site-directed mutagenesis. *Eur. J. Biochem.* **217**, 281–287.
18. Johnson, K. A., Chen, L., Yang, H., Roberts, M. F. & Stec, B. (2001). Crystal structure and catalytic mechanism of the MJ0109 gene product: a bifunctional enzyme with inositol monophosphatase and fructose 1,6-bisphosphatase activities. *Biochemistry*, **40**, 618–630.
19. Mildvan, A. S. (1997). Mechanisms of signaling and related enzymes. *Proteins: Struct. Funct. Genet.* **29**, 401–416.
20. Wilkie, J., Cole, A. G. & Gani, D. (1995). 3-Dimensional interactions between inositol monophosphatase and its substrates, inhibitors and metal-ion cofactors. *J. Chem. Soc., Perkin Trans. 1*, **21**, 2709–2727.
21. Leech, A. P., Baker, G. R., Shute, J. K., Cohen, M. A. & Gani, D. (1993). Chemical and kinetic mechanism of the inositol monophosphatase reaction and its inhibition by Li^+. *Eur. J. Biochem.* **212**, 693–704.
22. Otwinowski, Z. & Minor, W. (1997). Processing of X-ray diffraction data collected in oscillation mode. *Methods Enzymol.* **276**, 307–326.
23. Leslie, A. G. W. (1987). MOSFLM. In *Proceedings of the CCP4 Study* (Weekend, J. R., Machin, P. A. & Papiz, M. Z., eds), pp. 39–50, SERC Daresbury Laboratary, Warrinton, UK.
24. Collaborative Computing Project Number 4 (1994). The CCP4 suite: programs for protein crystallography. *Acta Crystallog. sect. D*, **50**, 760–763.
25. Kleywegt, G. J. & Jones, T. A. (1996). Phi/Psichology: Ramachandran revisited. *Structure*, **4**, 1395–1400.
26. Murshudov, G. N., Vagin, A. A. & Dodson, E. J. (1997). Refinement of macromolecular structures by the maximum-likelihood method. *Acta Crystallog. sect. D*, **53**, 240–255.
27. Jones, T. A., Zou, J. Y., Cowan, S. W. & Kjeldgaard, M. (1991). Improved methods for model building in electron density maps and the location of errors in these models. *Acta Crystallog. sect. A*, **47**, 110–119.
28. Perrakis, A., Sixma, T. K., Wilson, K. S. & Lamzin, V. S. (1997). wARP: improvement and extension of crystallographic phases by weighted averaging of multiple refined dummy atomic models. *Acta Crystallog. sect. D*, **53**, 448–455.
29. Laskowski, R. A., Macarthur, M. W., Moss, D. S. & Thornton, J. M. (1993). PROCHECK—a program to check the stereochemical quality of protein structures. *J. Appl. Crystallog.* **26**, 283–291.
30. Rodriguez, R., Chinea, G., Lopez, N., Pons, T. & Vriend, G. (1998). Homology modelling, model and software evaluation: three related resources. *Bioinformatics*, **14**, 523–528.
31. Kraulis, P. J. (1991). MOLSCRIPT: a program to produce both detailed and schematic plots of protein structures. *J. Appl. Crystallog.* **24**, 946–950.
32. Merritt, E. A. & Murphy, M. E. P. (1994). Raster3D version-2.0: a program for photorealistic molecular graphics. *Acta Crystallog. sect. D*, **50**, 869–873.
33. Diederich, K. & Karplus, P. A. (1997). Improved *R*-factors for diffraction data analysis in macromolecular crystallography. *Nature Struct. Biol.* **4**, 269–275.

Edited by R. Huber

(Received 26 February 2002; received in revised form 5 June 2002; accepted 5 June 2002)